22.101 Applied Nuclear Physics (Fall 2006)

Lecture 15 (11/6/06)

Charged-Particle Interactions: Radiation Loss, Range

References:

R. D. Evans, *The Atomic Nucleus* (McGraw-Hill, New York, 1955), Chaps 18-22.

W. E. Meyerhof, *Elements of Nuclear Physics* (McGraw-Hill, New York, 1967).

The sudden deflection of an electron by the Coulomb field of nuclei can cause the electron to radiate, producing a continuous spectrum of x-rays called *bremsstrahlung*. The fraction of electron energy converted into bremsstrahlung increases with increasing electron energy and is greater for media of high atomic number. (This process is important in the production of x-rays in conventional x-ray tubes.)

According to the classical theory of electrodynamics [J. D. Jackson, *Classical Electrodynamics* (Wiley, New York, 1962), p. 509], the acceleration produced by a nucleus of charge Ze on an incident particle of charge ze and mass M is proportional to Zze^2/M. The intensity of radiation emitted is proportional to (ze × acceleration)^2 ~ $(Zz^2e^3/M)^2$. Notice the $(Z/M)^2$ dependence; this shows that *bremsstrahlung* is more important in a high-Z medium. Also it is more important for electrons and positrons than for protons and α -particles. Another way to understand the $(Z/M)^2$ dependence is to recall the derivation of stopping power in Lec13 where the momentum change due to a collision between the incident particle and a target nucleus is $(2ze^2/vb)$ x Z. The factor Z represents the Coulomb field of the nucleus (in Lec13 this was unity since we had an atomic electron as the target). The recoil velocity of the target nucleus is therefore proportional to Z/M, and the recoil energy, which is the intensity of the radiation emitted, is therefore proportional to $(Z/M)^2$.

In an individual deflection by a nucleus, the electron can radiate any amount of energy up to its kinetic energy T. The spectrum of *bremsstrahlung* wavelength for a thick target is of the form sketched below, with $\lambda_{\min} = hc/T$. This converts to a frequency spectrum which is a constant up the maximum frequency of $\nu_{\max} = T/h$. The

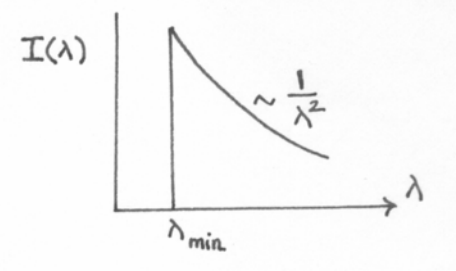

shape of the spectrum is independent of Z, and the intensity varies with electron energy like 1/T.

In the quantum mechanical theory of *bremsstrahlung* a plane wave representing the electron enters the nuclear field and is scattered. There is a small but finite chance that a photon will be emitted in the process. The theory is intimately related to the theory of pair production where an electron-positron pair is produced by a photon in the field of a nucleus. Because a radiative process involves the coupling of the electron with the electromagnetic field of the emitted photon, the cross sections for radiation are of the order of the fine-structure constant [Dicke and Wittke, p. 11], $e^2/\hbar c$ (= 1/137), times the cross section for elastic scattering. This means that most of the deflections of electrons by atomic nuclei result in elastic scattering, only in a small number of instances is a photon emitted. Since the classical theory of *bremsstrahlung* predicts the emission of radiation in every collision in which the electron is deflected, it is incorrect. However, when averaged over all collisions the classical and quantum mechanical cross sections are of the same order of magnitude,

$$\sigma_{rad} \sim \frac{Z^2}{137}\left(\frac{e^2}{m_e c^2}\right)^2 \quad \text{cm}^2/\text{nucleus} \qquad (14.1)$$

where $e^2/m_e c^2 = r_e = 2.818 \times 10^{-13}$ cm is the classical radius of electron. In the few collisions where photons are emitted a relatively large amount of energy is radiated. In this way the quantum theory replaces the multitude of small-energy losses predicted by the classical theory by a much smaller number of larger-energy losses. The spectral

distributions are therefore different in the two theories, with the quantum description being in better agreement with experiments.

Given a nucleus of charge Ze and an incident electron of kinetic energy T, the quantum mechanical differential cross section for the emission of a photon with energy in $d(h\nu)$ about $h\nu$ is

$$\left[\frac{d\sigma}{d(h\nu)}\right]_{rad} = \sigma_o B Z^2 \frac{T + m_e c^2}{T}\frac{1}{h\nu} \tag{14.2}$$

where $\sigma_o = \left(e^2 / m_e c^2\right)^2 / 137 = 0.580 \text{ x } 10^{-3}$ barns and B ~ 10 is a very slowly varying dimensionless function of Z and T. A general relation between the energy differential cross section, such as (14.2), and the energy loss per unit path length is

$$-\frac{dT}{dx} = n\int_0^T dE E\frac{d\sigma}{dE} \tag{14.3}$$

where $d\sigma / dE$ is the differential cross section for energy loss E. Applying this to (14.2) we have

$$-\left(\frac{dT}{dx}\right)_{rad} = n\int_0^T d(h\nu) h\nu \left[\frac{d\sigma}{d(h\nu)}\right]_{rad}$$

$$= n(T + m_e c^2)\sigma_{rad} \qquad \text{ergs/cm} \tag{14.4}$$

where $$\sigma_{rad} = \sigma_o Z^2 \int_0^1 d\left(\frac{h\nu}{T}\right) B \equiv \sigma_o Z^2 \overline{B} \tag{14/5}$$

is the total *bremsstrahlung* cross section. The variation of $\bar{B}$, the *bremmstrahlung* cross section in units of $\sigma_o Z^2$, with the kinetic energy of an incident electron is shown in the sketch for media of various Z [Evans, p. 605].

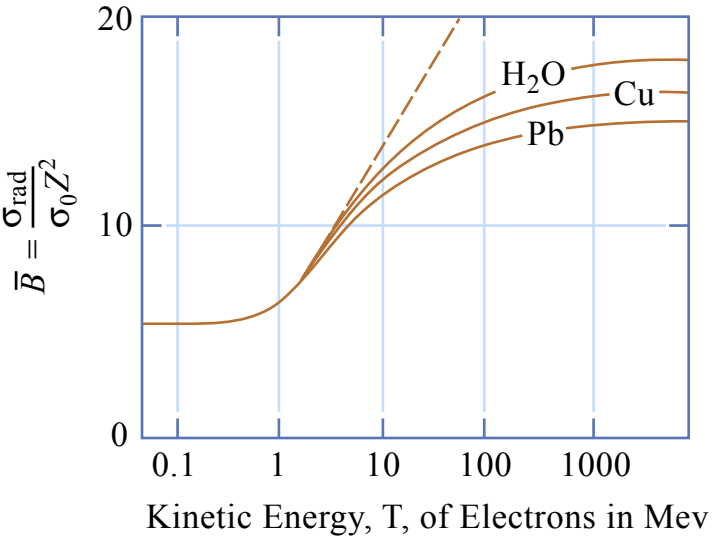

Figure by MIT OCW. Adapted from Evans.

Comparison of Various Cross Sections

It is instructive to compare the cross sections describing the interactions that we have considered between an incident electron and the atoms in the medium. For nonrelativistic electrons, T $\leq$ 0.1 Mev and $\beta \quad v/c \leq 0.5$, we have the following cross sections (all in barns/atom) [Evans, p. 607],

$$\sigma_{ion} = \frac{2\alpha Z}{\beta^4} \ell n\left(\frac{\sqrt{2}T}{\bar{I}}\right) \qquad \text{ionization} \qquad (14.6)$$

$$\sigma_{nuc} = \frac{\alpha Z^2}{4\beta^4} \qquad \text{backscattering by nuclei} \qquad (14.7)$$

$$\sigma_{el} = \frac{2\alpha Z}{\beta^4} \qquad \text{elastic scattering by atomic electrons} \qquad (14.8)$$

$$\sigma'_{rad} = \frac{8\alpha}{3\pi}\frac{1}{137}\frac{Z^2}{\beta^2} \qquad \textit{bremsstrahlung} \qquad (14.9)$$

where $\alpha = 4\pi(e^2/m_e c^2)^2$ = 1.00 barn. The values of these cross sections in the case of 0.1 Mev electrons in air (Z = 7.22, $\bar{I}$ ~ 100 ev) and in Pb (Z = 82, $\bar{I}$ ~ 800 ev) are given in the following table [from Evans, p.608]. The difference between σ_{rad} and σ'_{rad} is that the former corresponds to fractional loss of *total* energy, $dT/(T + m_e c^2)$, while the latter corresponds to fractional loss of *kinetic* energy, dT/T.

Approximate Cross Sections in Barns per Atom of Pb, and of Air, for Incident 0.1-Mev Electrons

	Ionization	Nuclear elastic backward scattering $\nu \geq 90^o$	Electronic (inelastic) scattering $\nu \geq 45^o$	Bremsstrahlung	
				σ_{rad}	σ'_{rad}
Approximate variation with Z and β	Z/β^4	Z^2/β^4	Z/β^4	Z^2	Z^2/β^2
Air.....	1,200	150	160	0.16	1.0
Pb.....	9,400	19,000	1,800	21	130

Figure by MIT OCW. Adapted from Evans.

Mass Absorption

Ionization losses per unit distance are proportional to nZ, the number of atomic electrons per cm^3 in the absorber (medium). We can express nZ as

$$nZ = (\rho N_o / A)Z = \rho N_o (Z/A) \qquad (14.10)$$

where ρ is the mass density, g/cm^3, and N_o the Avogadro's number. Since the ratio (Z/A) is nearly a constant for all elements, it means that nZ/ρ is also approximately constant (except for hydrogen). Therefore, if the distance along the path of the charged particle is measured in units of $\rho dx \equiv dw$ (in g/cm^2), then the ionization losses, -dT/dw (in ergs cm^2/g) become more or less independent of the material. We see in Fig. 14.1, the expected behavior of energy loss being material independent holds only approximately,

as -dT/dw actually decreases as Z increases. This is due to two reasons, Z/A decreasing slightly as Z increases and $\bar{I}$ increasingly linearly with Z.

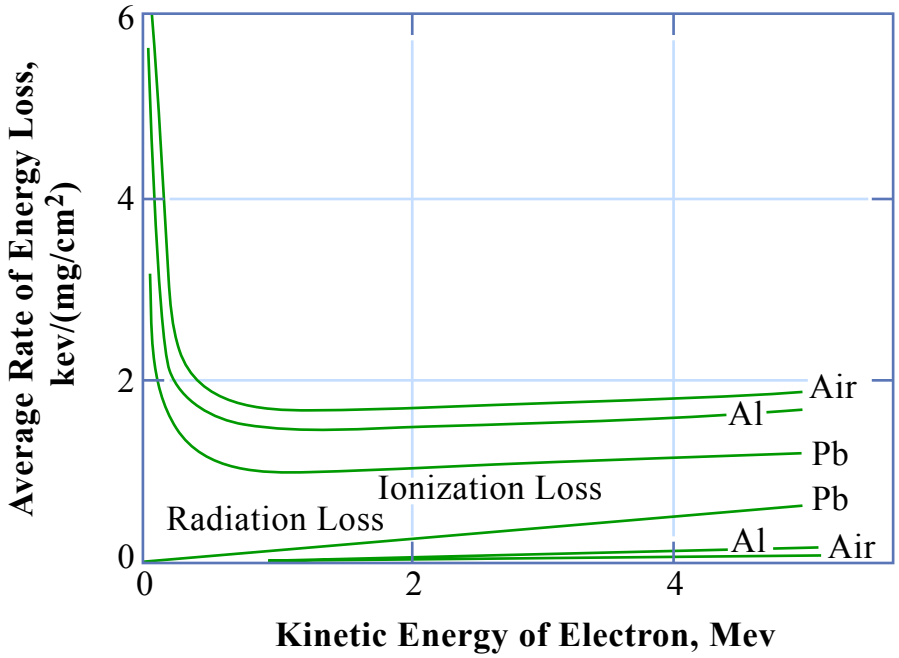

Figure by MIT OCW. Adapted from Evans.

Fig. 14.1. Mass absorption energy losses, -dT/dw, for electrons in air, Al, and Pb, ionization losses (upper curves) versus bremsstrahlung (lower curves). All curves refer to energy losses along the actual path of the electron. [Evans, p.609]

We have seen that ionization losses per path length vary mainly as $1/v^2$ while radiative losses increase with increasing energy. The two become roughly comparable when $T >> Mc^2$, or $T >> m_e c^2$ in the case of electrons. The ratio can be approximately expressed as

$$\frac{(dT/dx)_{rad}}{(dT/dx)_{ion}} \approx Z\left(\frac{m_e}{M}\right)^2\left(\frac{T}{1400 m_e c^2}\right) \qquad (14.11)$$

where for electrons, $M \rightarrow m_e$. The two losses are therefore equal in the case of electrons for $T = 18\ m_e c^2 = 9$ Mev in Pb and $T \sim 100$ Mev in water or air.

Range, Range-Energy Relations, and Track Patterns

When a charged particle enters an absorbing medium it immediately interacts with the many electrons in the medium. For a heavy charged particle the deflection from

any individual encounter is small, so the track of the heavy charged particle tends to be quite straight except at the very end of its travel when it has lost practically all its kinetic energy. In this case we can estimate the range of the particle, the distance beyond which it cannot penetrate, by integrating the stopping power,

$$R = \int_0^R dx = \int_{T_o}^{0} \left(\frac{dx}{dT} \right) dT = \int_0^{T_o} \left(-\frac{dT}{dx} \right)^{-1} dT \tag{14.12}$$

where T_o is the initial kinetic energy of the particle. An estimate of R is given by taking the Bethe formula, (13.7), for the stopping power and ignoring the v-dependence in the logarithm. Then one finds

$$R \propto \int_0^{T_o} T dT \; = \; T_o^2 \tag{14.13}$$

This is an example of a range-energy relation. Given what we have said about the region of applicability of (13.7) one might expect this behavior to hold at low energies. At high energies it is more reasonable to take the stopping power to be a constant, in which case

$$R \propto \int_0^{T_o} dT \; = T_o \tag{14.14}$$

We will return to see whether such behavior are seen in experiments.

Experimentally one can determine the energy loss by the number of ion pairs produced from an ionization event. The amount of energy W required for a particle of certain energy to produce an ion pair is known. The number of ion pairs, i, produced per unit path length (*specific ionization*) of the charged particle is then

$$i = \frac{1}{W} \left(-\frac{dT}{dx} \right) \tag{14.15}$$

The quantity W depends on complicated processes such as atomic excitation and secondary ionization in addition to primary ionization. On the other hand, for a given material it is approximately independent of the nature of the particle or its kinetic energy. For example, in air the values of W are 35.0, 35.2, and 33.3 ev for 5 kev electrons, 5.3 Mev alphas, and 340 Mev protons respectively.

The specific ionization is an appropriate measure of the ionization processes taking place along the path (track length) of the charged particle. It is useful to regard (14.15) as a function of the distance traveled by the particle. Such results can be seen in Fig. 14.2, where one sees a characteristic shape of the ionization curve for a heavy charged particle. Ionization is constant or increasing slowly during the early to mid stages of the total travel, then it rises more quickly and reaches a peak value at the end of the range before dropping sharply to zero.

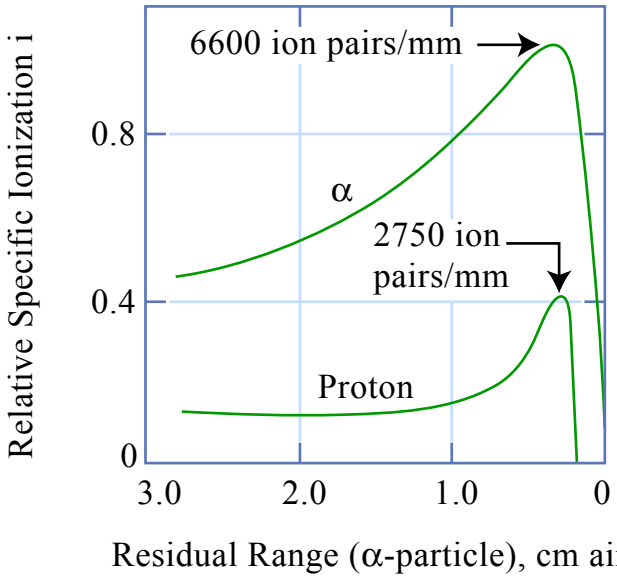

Figure by MIT OCW. Adapted from Meyerhof.

Fig. 14.2. Specific ionization of heavy particles in air. Residual range refers to the distance still to travel before coming to rest. Proton range is 0.2 cm shorter than that of the α-particle [Meyerhof, p.80].

We have already mentioned that as the charged particle loses energy and slows down, the probability of capturing electron increases. So the mean charge of a beam of particles will decrease with the decrease in their speed (cf. Fig. 13.3). This is the reason why the specific ionization shows a sharp drop. The value of –dT/dx along a particle track is also called specific energy loss. A plot of –dT/dx along the track of a charged particle is known as a Bragg curve. It should be emphasized that a Bragg curve differs

from a plot of –dT/dx for an individual particle in that the former is an average over a large number of particles. Hence the Bragg curve includes the effects of straggling (statistical distribution of range values for particles having the same initial velocity) and has a pronounced tail beyond the extrapolated range as can be seen in Fig. 14.3.

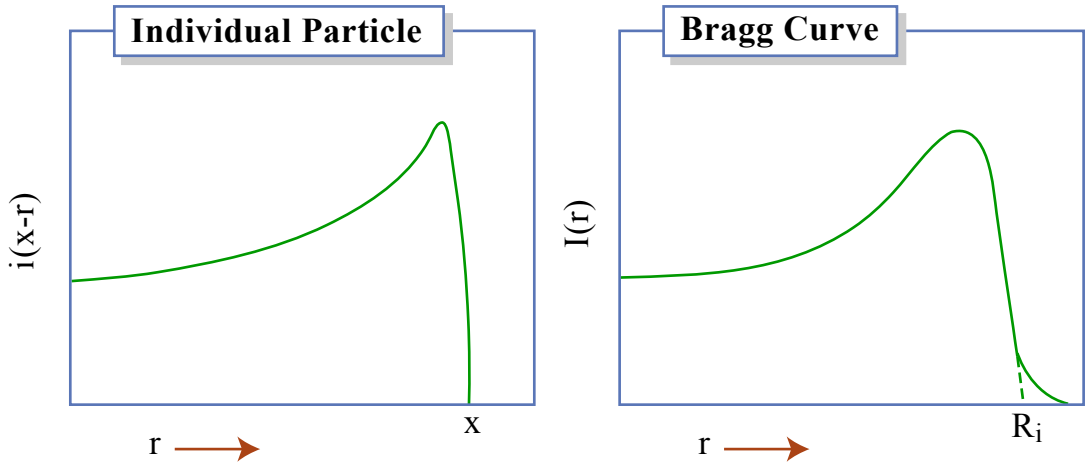

Figure by MIT OCW. Adapted from Evans.

Fig. 14.3. Specific ionization for an individual particle versus Bragg curve [Evans, p. 666].

A typical experimental arrangement for determining the range of charged particles is shown in Fig. 14.4. The mean range $\bar{R}$ is defined as the absorber thickness at which the intensity is reduced to one-half of the initial value. The extrapolated range R_o is obtained by linear extrapolation at the inflection point of the transmission curve. This is an example that I/Io is not always an exponential. In charged particle interactions it is not sufficient to think of $I / I_o = e^{-\mu x}$, one should be thinking about the range R.

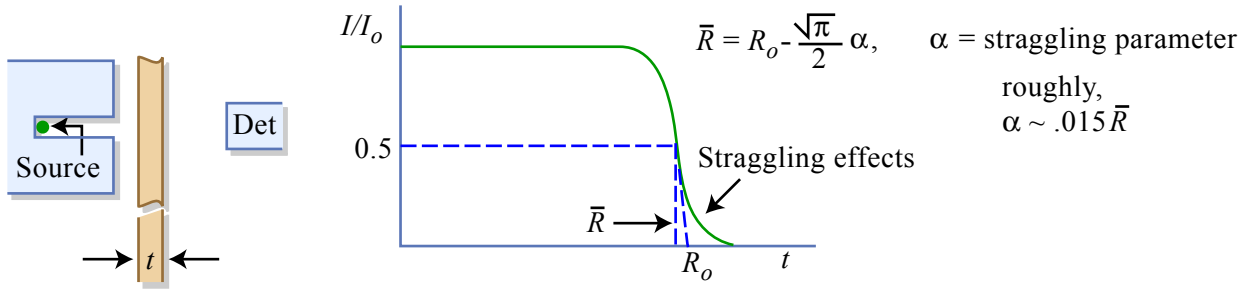

Figure by MIT OCW. Adapted from Knoll.

An alpha particle transmission experiment. I is the detected number of alphas through an absorber thickness t, whereas I^o is the number detected without the absorber. The mean range R and extrapolated range R^o are indicated.

Fig. 14.4. Determination of range by transmission experiment [from Knoll].

In practice one uses range-energy relations that are mostly empirically determined. For a rough estimate of the range one can use the Bragg-Kleeman rule,

$$\frac{R}{R_1} = \frac{\rho_1 \sqrt{A}}{\rho \sqrt{A_1}} \tag{14.16}$$

where the subscript 1 denotes the reference medium which is conventionally taken to be air at 15°C, 760 mm Hg ($\sqrt{A_1} = 3.81$, $\rho_1 = 1.226 \times 10^{-3}$ g/cm^3). Then

$$R = 3.2x10^{-4} \frac{\sqrt{A}}{\rho} \text{ x } R_{air} \tag{14.17}$$

with ρ in g/cm^3. In general such an estimate is good to within about $\pm$ 15 percent. Figs. 14.5 and 14.6 show the range-energy relations for protons and α-particles in air respectively. Notice that at low energy the variation is quadratic, as predicted by (14.13), and at high energy the relation is more or less linear, as given by (14.14). The same trend is also seen in the results for electrons, as shown in Fig. 14.7.

Fig. 14.5. Range-energy relations of α-particles in air [Evans, p. 650].

Fig. 14.6. Range-energy relation for protons in air [Evans, p. 651].

Fig. 14.7. Range-energy relation for electrons in aluminum [Evans, p. 624].

We have mentioned that heavy charged particles traverse essentially in a straight line until reaching the end of its range where straggling effects manifest. In the case of

electrons large deflections are quite likely during its traversal, so the trajectory of electron in a thick absorber is a series of zigzag paths. While one can still speak of the range R, the concept of path length is now of little value. This is illustrated in Figs. 14.8 and 14.9. The total path length S is appreciably greater than the range R

Image removed due to copyright restrictions.
Please see Figure 1.1 in Evans. p. 612

Fig. 14.8. Distinction between total path length S and range R [Evans, p. 612]

Image removed due to copyright restrictions.
Please see Figure 1.2 in Evans. p. 612

Fig. 14.9. Comparing distributions of total path length and range for electrons in oxygen [Evans, p. 612].

The transmission curve I/I_o for a heavy charged particle was shown in Fig. 14.4. The curve has a different characteristic shape for monoenergetic electrons, as indicated in Fig. 14.10, and a still different shape for β-rays (electrons with a distribution of energies), seen in Fig. 14.11. Although the curve for monoenergetic electrons depends to some extent on experimental arrangement, one may regard it as roughly a linear variation which is characteristic of single interaction event in removing the electron. That is, the fraction of electrons getting through is proportional to 1 – P, where P is the interaction probability which is in turn proportional to the thickness. For the β-ray transmission curve which essentially has the form of an exponential, the shape is an accidental consequence of the β-ray spectrum and of the differences between the scattering and absorption of electrons which have various initial energies [cf. Evans, p. 625]. It is found empirically that R_m is the same as R_o if the monoenergetic electrons are given the energy $E = E_{max}$, the maximum energy of the β-ray spectrum (the end-point energy).

Fig. 14. 10. Transmission curve of monoenergetic electrons (sensitive to experimental arrangement) [Evans, p. 623].

Image removed due to copyright restrictions.
Please see Figure 3.4 in Evans. p. 625

Fig. 14.11. Transmission curve for β-rays [Evans, p.625].

Cerenkov Radiation

Electromagnetic radiation is emitted when a charged particle passes through a medium under the condition

$$v_{group} \equiv \beta c > v_{phase} \equiv c/n \qquad (14.15)$$

where n is the index of refraction of the medium. When $\beta n > 1$, there is an angle (a direction) where constructive interference occurs. This radiation is a particular form of energy loss, due to soft collisions, and is not an additional amount of energy loss. Soft collisions involve small energy transfers from charged particles to distant atoms which become excited and subsequently emit coherent radiation (see Evans, p. 589).